

FZD-499

## Thermal Analysis of EPOS components

M. Werner, E. Altstadt, M. Jungmann,  
G. Brauer, K. Noack, A. Rogov  
R. Krause-Rehberg

Juni 2008

Wissenschaftlich-Technische Berichte  
FZD-499 2008 · ISSN 1437-322X

WISSENSCHAFTLICH-TECHNISCHE BERICHTE



Forschungszentrum  
Dresden Rossendorf

M. Werner, E. Altstadt , M. Jungmann, G. Brauer, K. Noack,  
A. Rogov, R. Krause-Rehberg

## **Thermal Analysis of EPOS components**

Abstract:

We present a simulation study of the thermal behaviour of essential parts of the electron-positron converter of the positron source EPOS at the Research Center Dresden-Rossendorf. The positron moderator foil and the upper tube element of the electrostatic extraction einzelens are directly exposed to the primary electron beam (40 MeV, 40 kW). Thus, it was necessary to prove by sophisticated simulations that the construction can stand the evolving temperatures. It was found that thin moderator foils ( $< 20...40 \mu\text{m}$ ) will not show a too strong heating. Moreover, the temperature can be varied in a wide range by choosing an appropriate thickness. Thus, the radiation-induced lattice defects can at least partly be annealed during operation. The wall of the extraction lens which is made from a stainless steel tube must be distinctly thinned to avoid damage temperatures. The simulations were performed time dependent. We found that the critical parts reach their final temperature after less than a minute.

**Contents**

1	Introduction .....	4
2	Evaluation of the heat generation rates .....	5
3	Thermal calculations .....	7
3.1	Model.....	7
3.2	Material properties.....	8
3.3	Load and boundary conditions .....	9
3.4	Results .....	9
3.4.1	Temperature in the moderator .....	10
3.4.2	Temperatures in the lens .....	11
4	Conclusions .....	15
	References .....	15

## 1 Introduction

The positron beam technique is a unique tool to study crystal lattice defects and open-volume cavities of nanometres scale in thin samples and layers [1].

The superconducting electron LINAC **ELBE** (**E**lectron **L**inac with high **B**rilliance and low **E**mittance) at Forschungszentrum Dresden-Rossendorf [2] gives the unique possibility to construct an intense, pulsed positron beam line for materials research. The positron beam will be bunched for positron lifetime spectroscopy by making use of the primary bunch structure of the ELBE electron beam (77 ns repetition time of 5 ps bunches, cw-mode, 40 MeV, 1 mA average current).

A detailed description of the ambitious intentions to realize the EPOS project has already been published [3]. However, this realization is not straightforward and sometimes several options have to be considered and tested before a reasonable solution to a certain problem is found. The present report reviews activities with respect to the thermal analysis of EPOS components. Such efforts are essential for an efficient choice of construction materials.

In particular, this report analyses the thermal behaviour of the positron moderator and the electrostatic lenses designed in such a way that a mono-energetic positron beam can be formed for transportation into the positron laboratory. This analysis is necessary because both parts will be hit by the intense primary electron beam which is strongly broadened when passing the Bremstrahlung-converter consisting of a stack of fifty 100 $\mu$ m-tungsten foils. This electron beam is still very energetic even after passing the converter. Earlier simulations [3] have shown that about 14 kW must be dissipated in the electron-positron converter and 21 kW in the beam dump. The energy deposition and thus the temperature of the tungsten moderator and the upper piece of the stainless-steel lens tube is, however, adjustable by choosing the thickness of the material (Fig. 1).

The aim of this thermal analysis was, therefore, to find a suitable material geometry to avoid a too strong thermal heat load. In a first step, the volumetric heat generation is calculated using the code MCNP. In a second step, the time dependent temperature distributions are evaluated using the finite element code ANSYS. Figure 1 shows the configuration under consideration.

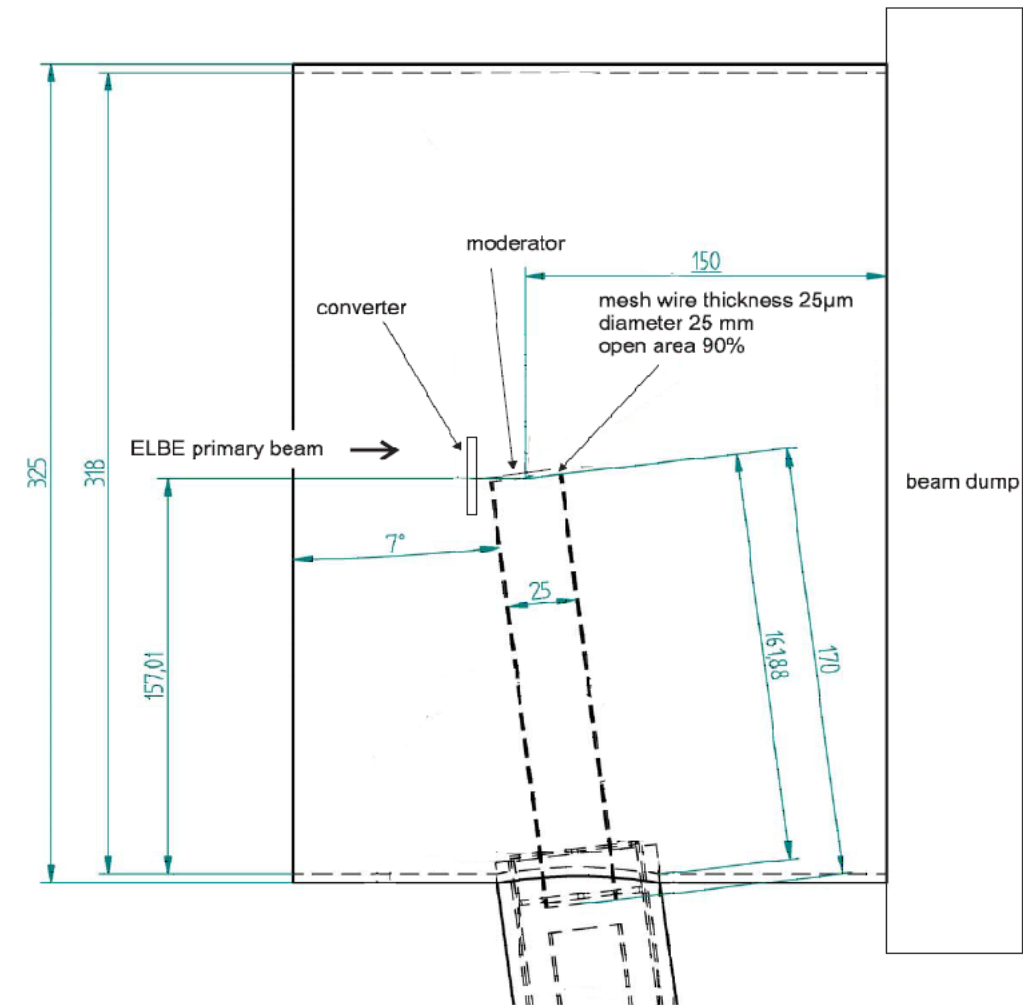


**Figure 1:** Part of the EPOS configuration. The ELBE electron beam hits the electron-gamma converter and is broadened from 5mm diameter to an angle so that the whole beam dump is exposed. The positron moderator (20 μm tungsten foil) is placed in front of the converter and parallel to the entrance plane of the upper tube of the positron focusing lens (see Fig. 2).

## 2 Evaluation of the heat generation rates

The heat generation rates in the moderator and upper lens tube were calculated with the Monte Carlo code MCNP<sup>®</sup>-5, release 1.40 [4]. MCNP is a general-purpose Monte Carlo N-Particle code that can be used for stochastically simulating neutron, photon, electron, or coupled neutron/photon/electron transports. The code is able to treat an arbitrary three-dimensional configuration of materials. For neutrons and photons energy point wise cross-section data given in Evaluated Nuclear Data Libraries (such as ENDF/B-VI) are used to account for the various interactions with the materials. In case of electrons they are treated by means of a continuous-slowing-down model. The code allows the estimation of a broad range of integrals of the space-, energy- and direction-dependent particle fields together with their statistical errors. For the study presented in this report the mean values of the heat generation by photons and electrons averaged over user-defined volumes were calculated in a coupled electron/photon/neutron transport simulation. Contributions from neutrons to the heat generation are negligible.

Figures 2 and 3 show the arrangement and the definition of the estimation volumes (cells). The moderator foil was chosen to have a homogenous thickness of 20  $\mu\text{m}$  (cell 202). The electrostatic lens consists of 3 tubes. Only the upper lens tube is hit by the electron beam. Thus, only this tube is taken into the consideration and is shown in Figs. 1 and 2. The lens tube having a wall thickness of 1 mm (cell 241) is in the upper part, which is exposed to the high-energetic electron beam electrochemically thinned to a wall thickness of 50  $\mu\text{m}$  (cell 210, 220 and 230 to 236). On top of this tube an electrostatic extraction grid of stainless steel is welded (cell 243).

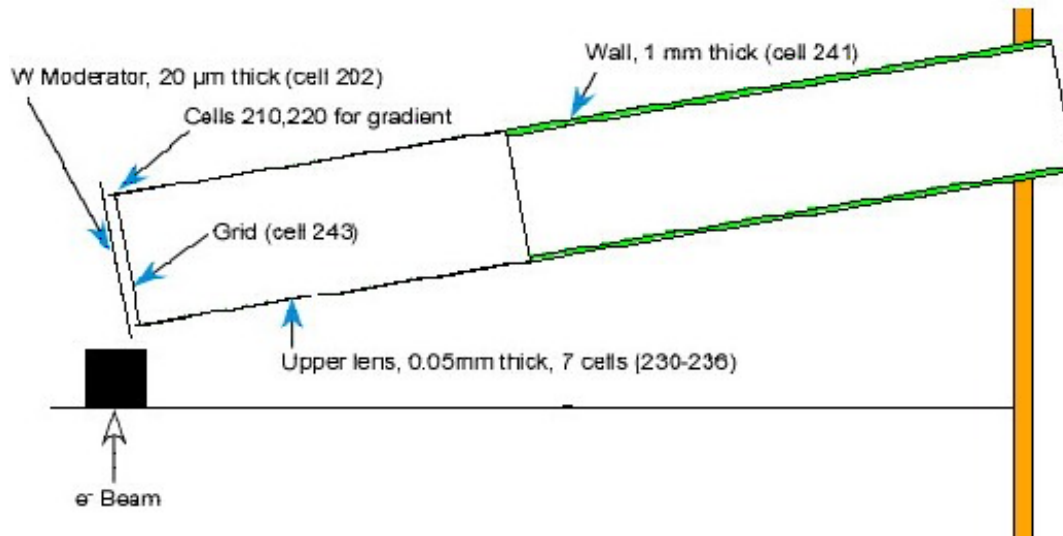


**Figure 2:** Arrangement of the upper tube piece of the electrostatic lens and the moderator. The definition of the MCNP cells is indicated.

The results of the calculation for the different cells are listed in Table 1. The energy input values are given as integral values in the volumes  $V_i$  for one electron with an energy of 40 MeV.

**Table 1:** Results of the energy input calculation

Cell	Volume $V_i$ [ $\text{cm}^3$ ]	Mass [g]	Energy input $E_i$ [MeV]	Rel. stat. error [-]	Comment
202	1.414e-2	2.714e-1	1.18e-2	0.0028	W-moderator, complete
210	3.000e-4	2.304e-3	5.77e-5	0.0223	additional cells to account for the gradient in beam direction
220	3.000e-4	2.304e-3	2.42e-4	0.0147	
230	3.919e-2	3.010e-1	9.10e-3	0.0031	ring 1, height 1 cm
231	3.919e-2	3.010e-1	4.26e-3	0.0044	ring 2, height 1 cm
232	3.919e-2	3.010e-1	2.28e-3	0.0062	ring 3, height 1 cm
233	3.919e-2	3.010e-1	1.37e-3	0.0081	ring 4, height 1 cm
234	3.919e-2	3.010e-1	8.84e-4	0.0104	ring 5, height 1 cm
235	3.919e-2	3.010e-1	6.09e-4	0.0122	ring 6, height 1 cm
236	3.919e-2	3.010e-1	4.28e-4	0.0175	ring 7, height 1 cm
241	7.389e+0	5.675e+1	1.88e-2	0.0063	lower part of the lens
243	1.461e-3	1.122e-2	5.32e-4	0.0086	grid at the top of the lens

The volumetric heat generation is obtained by:

$$Q_i^{\text{vol}} = \frac{E_i}{V_i} \cdot I/e \quad \text{Eq 1}$$

where  $I$  is the current of the electron beam and  $I/e$  equals the number of electrons per seconds.

### 3 Thermal calculations

#### 3.1 Model

Based on the code ANSYS® a finite element model is used to calculate the transient temperature distribution in the moderator, the grid and in the positron lens. Heat conduction within the materials and radiation heat transfer at the surfaces are considered. The heat generation density is obtained from Table 1. An axisymmetric model was chosen assuming that the temperature gradient in beam direction is negligible. To be conservative with respect to the maximum temperature, the greater value of the heat generations in the additional cells 210 and 220 was added in the upper region of ring 1 (cf. Table 1). Figure 3 shows the scheme of the model (not to scale). The heat conduction and the volumetric heat input is realised by the ANSYS element type PLANE55 (black) whereas the element type SURF151 is used for the heat radiation (red lines). Surfaces that are not meshed with SURF151 are adiabatic. The Fe model consists of 2362 elements and 2335 nodes.



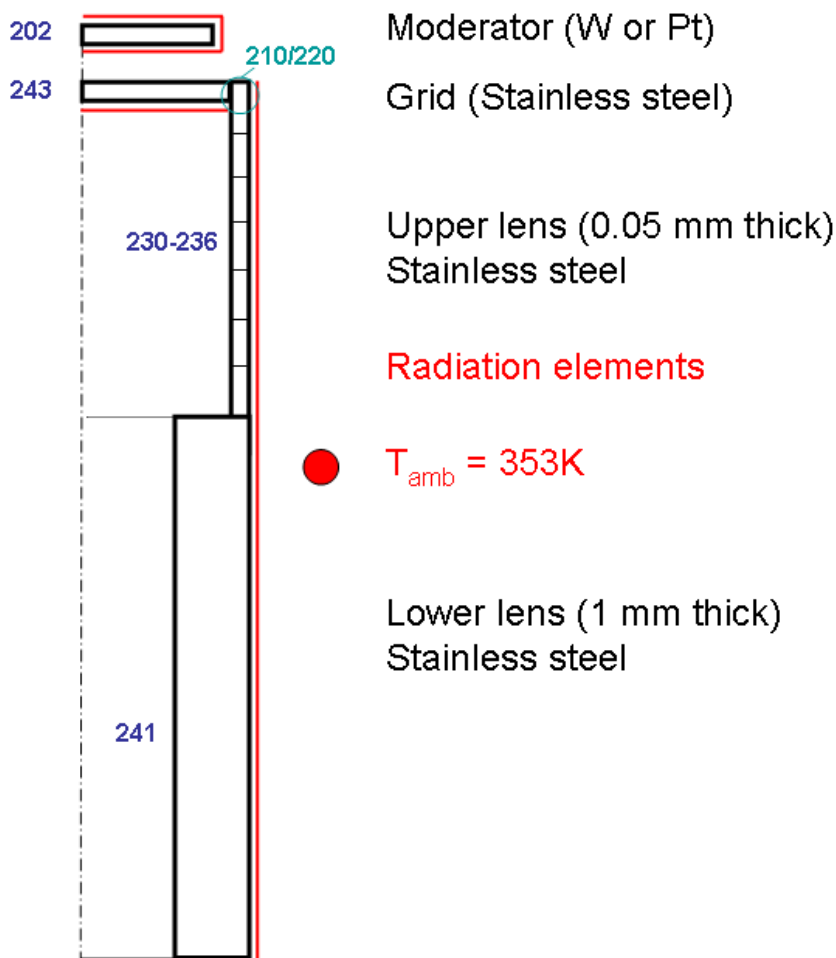


**Figure 3:** Scheme of the axisymmetric FE-model with indication of the MCNP cell numbers

### 3.2 Material properties

The lens and the grid are made of stainless steel. For the positron moderator two material options are considered: Pt and W. The extraction grid has an opening of 90%. To take this fact into account in the model reduced (or effective) material constants are used. The following material properties were used (Table 2):

**Table 2:** Material properties for the thermal analysis

Material	Tungsten (W)	Platinum (Pt)	Steel	Steel (grid)
Density [kg/m <sup>3</sup> ]	19259	21450	7800	780
Heat conduction coef. [W/m/K]	174	71.6	15	1.5
Specific heat [J/kg/K]	130	133	510	51
Emission coef. [-]	$\varepsilon(T)$	$\varepsilon(T)$	0.24	0.24

Figure 4 and Figure 5 show the emission coefficients vs. T for tungsten and platinum respectively [5].

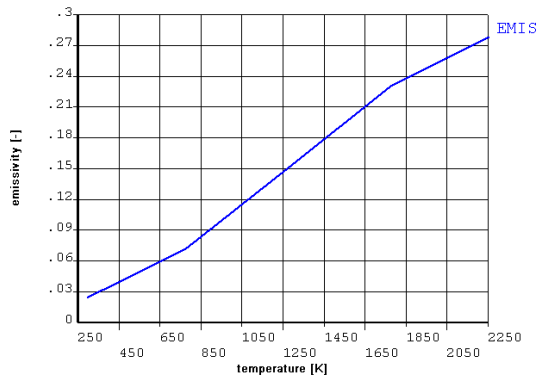


**Figure 4:** Emission coefficient of tungsten vs. temperature

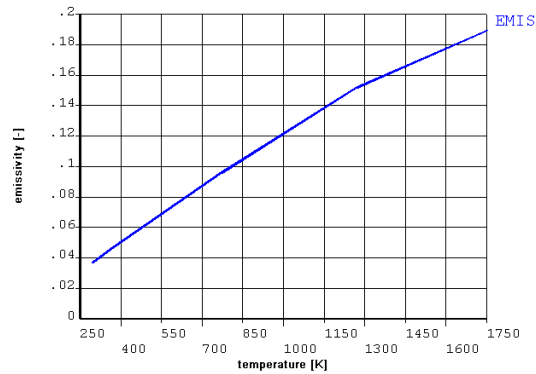


**Figure 5:** Emission coefficient of platinum vs. temperature

### 3.3 Load and boundary conditions

The volumetric heat generation density is obtained by converting the value of Table 1 using equation 1 assuming a current of  $I=1$  mA, thus a total electron power of 40kW. One obtains:

**Table 3:** Heat generation rates

Cell	Heat generation rate [W/m <sup>3</sup> ]	Comment
202	8.345E+8	moderator
220	8.067E+8	additional range for gradient (added to 230)
230	2.322E+8	upper part of lens (thickness 0.05 mm)
231	1.087E+8	
232	5.818E+7	
233	3.496E+7	
234	2.256E+7	
235	1.554E+7	
236	1.092E+7	
241	2.554E+6	lower part of lens (thickness 1 mm)
243	3.641E+8	grid

The volumetric heat sources are “switched on” at  $t=0$  and remain constant afterwards. The heat generation rates in Table 3 are valid for the full power mode. During the diagnostic mode 1% of these values are used. The initial temperature of the whole structure at  $t=0$  is  $T_0 = 308$  K = 25 °C, the ambient temperature is assumed to be constant  $T_a = 353$  K = 80 °C. For the volumetric heat generation rates in Pt we assumed the same values as in W.

### 3.4 Results

Transient calculations were performed for different scenarios. The following parameters were varied:

- the power of the beam (1% - diagnostic mode and 100% - full mode)
- the moderator material (W or Pt)
- the thickness of the moderator
- the heat generation in the grid (100% - upper bound; 10% - realistic case)

The calculations were stopped when a steady state temperature field was reached.

### 3.4.1 Temperature in the moderator

The heat-up of the moderator was calculated for Pt and W with a nominal thickness of 0.04 mm at 100% beam power. Figure 6 and Figure 7 show the maximum temperatures vs. time for W and Pt respectively.

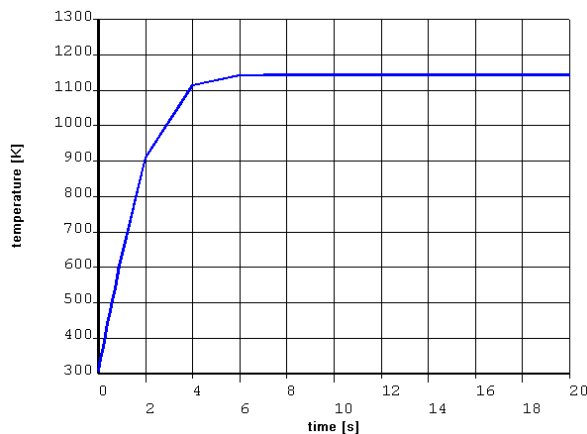


**Figure 6:** Temperature [K] vs. time [s] in the W moderator at 100% beam power

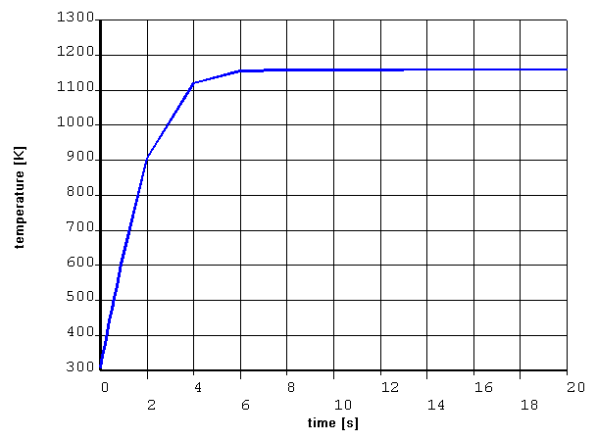


**Figure 7:** Temperature [K] vs. time [s] in the Pt moderator at 100% beam power

It can be seen that the steady state temperature is reached at about  $t = 8$  s in both cases. The final temperature in W is 1144 K and in Pt 1158 K. The somewhat smaller value in W correlates to the slightly larger emission coefficient at  $\sim 1000$  K.

In the following we investigate the influence of the moderator thickness on the maximum temperature. It is obvious that the maximum temperature will increase with increasing thickness, since the volume to surface ratio is given by:

$$\frac{V}{A_{\text{surf}}} = \frac{s}{2 + 4 \cdot s/D} \quad \text{Eq 2}$$

where  $s$  and  $D$  are thickness and diameter respectively ( $s \ll D$ ). The thickness should be chosen in such a way that:

- the maximum temperature is sufficiently far from the melting temperature of the material (W: 3683 K; Pt: 2045 K) and
- the maximum temperature is high enough to enable the healing of the microstructural point defects caused by the irradiation

The thickness of the moderator was varied from 0.01 mm to 0.7 mm for W and from 0.01 mm to 0.48 mm for Pt. The dependence of  $T_{\text{max}}$  on the thickness is shown in Figure 8. The total heat input, which is proportional to the thickness, is indicated in the upper horizontal axis.

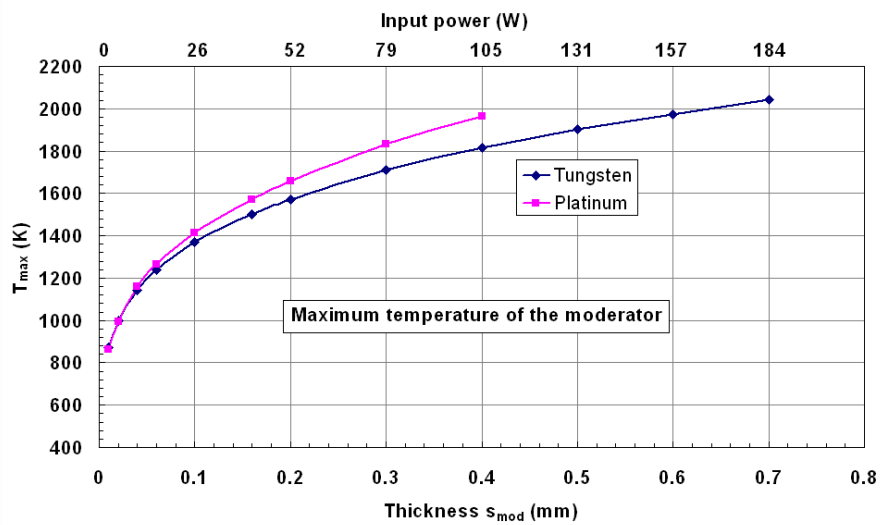


**Figure 8:** Maximum moderator temperature in dependence on thickness

The temperature gradient in the moderator is rather small. It depends on the thickness (cf. Table 4).

**Table 4:** Temperature gradient in the moderator: difference between maximum temperature (central point) and minimum temperature (surface) in the steady state

	W-moderator	Pt-moderator
Thickness	$T_{\max} - T_{\text{surf}}$	$T_{\max} - T_{\text{surf}}$
0.04 mm	0.42 K	0.43 K
0.1 mm	1.07 K	1.08 K
0.2 mm	2.16 K	2.19 K
0.3 mm	3.22 K	3.27 K
0.4 mm	4.28 K	4.34 K
0.5 mm	5.30 K	5.39 K

### 3.4.2 Temperatures in the lens

The temperature distributions in the lens (grid and tube) are discussed for the case of 1% and 100% heat generation.

For the upper border case the influence of the emission coefficient of steel is investigated in the range  $0.03 \leq \varepsilon_{\text{st}} \leq 1$ . The emission coefficient of steel strongly depends on the surface finishing; therefore the “nominal” value given in Table 2 might be inaccurate.

Figure 9 shows the temperature vs. time for 100% beam power at different locations. The steady state is reached after ~60 s. Figure 10 shows the steady state temperature distribution in the extraction tube.

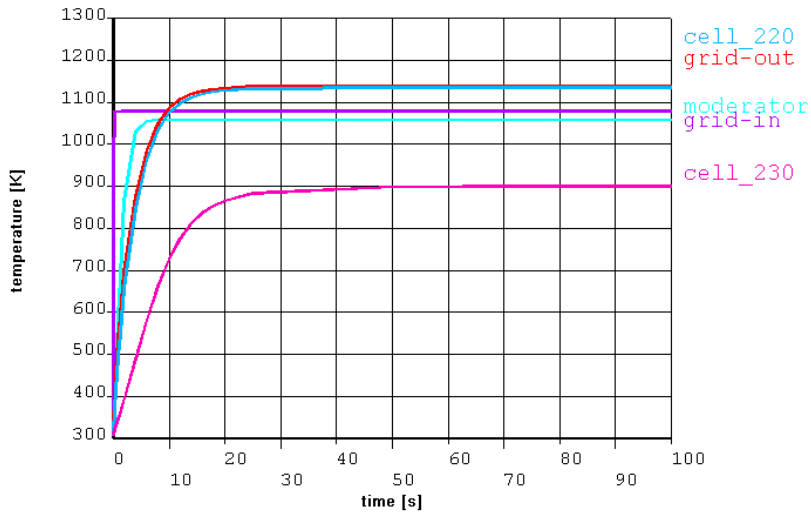


**Figure 9:** Temperature vs. time for different positions; 100% beam power, emission coefficient  $\varepsilon = 0.24$

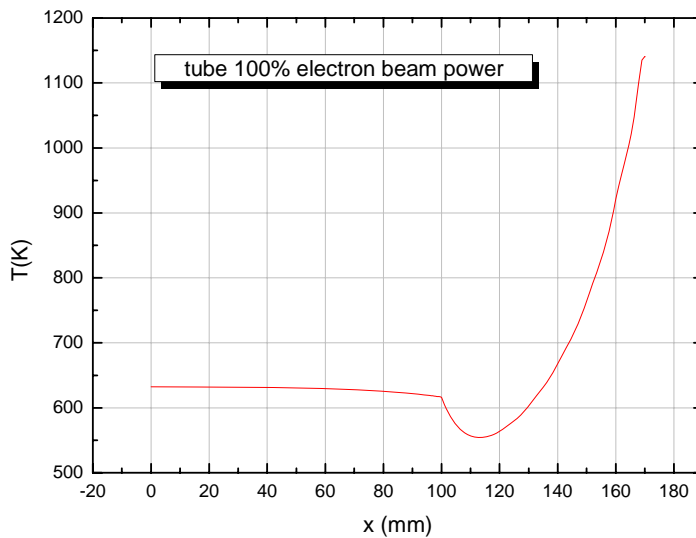


**Figure 10:** Temperature distribution [K] in the upper part of the extraction lens at  $t = 785$  s (100% beam power). The left part of the tube ( $x=0\dots 100$ mm) has the full thickness (1mm). The right part ( $x > 100$ mm) has been thinned to a thickness of  $50 \mu\text{m}$  to reduce the power loss in the tube.

The influence of the emission coefficient on the maximum (steady state) temperature is shown in Figure 11 and Figure 12. It can be seen that the hottest point is the end part where the grid is connected to the tube ("grid\_periph"). Here, the electron beam has the highest intensity.

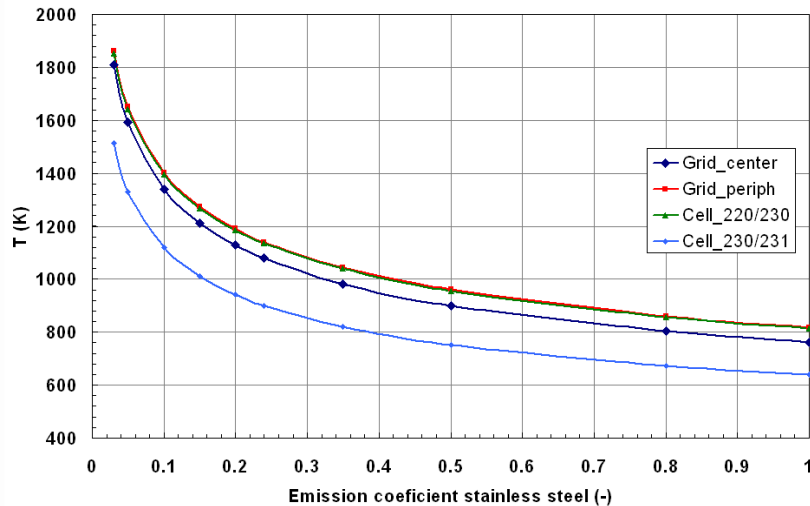


**Figure 11:** Maximum temperatures vs. emission coefficient at different positions in the upper part of the tube; 100% beam power

In the lower part of the tube (cell 241) the temperatures are significantly lower than in the upper part. It can be concluded that for  $\varepsilon \geq 0.05$  the maximum temperature in the tube is clearly lower than the melting temperature of steel ( $\sim 1760$  K).

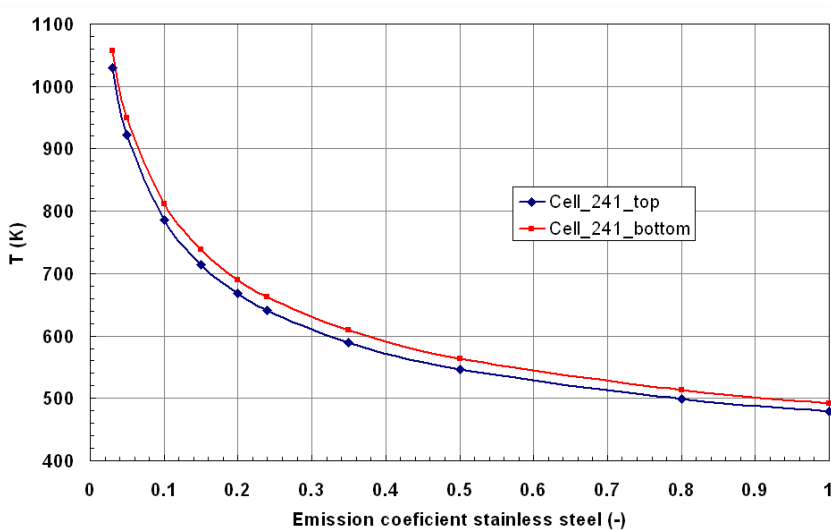


**Figure 12:** Maximum temperatures vs. emission coefficient at different positions in the lower part of the tube; 100% beam power

For the diagnostic mode the beam power is 1% of the nominal power. The volumetric heat generation rate is reduced likewise. The temperatures vs. time are shown in Figure 13 and Figure 14. The calculations were performed for the nominal emission coefficient of  $\varepsilon = 0.24$ . As expected the temperatures are much lower than with full beam power. The overall maximum is about  $409$  K =  $136$  °C. Fig 15 shows that the temperature of the extraction lens never exceeds 400K in diagnostic mode.

The mesh grid (90% mesh opening, 25  $\mu$ m thick stainless steel) is fixed by point welding on top of the upper tube of the extraction lens. The temperature varies according to our simulations between 1080 ... 1140 K at full power, and between 396

... 408 K at 1% beam power (not shown in a figure) and is thus also safe for this component.

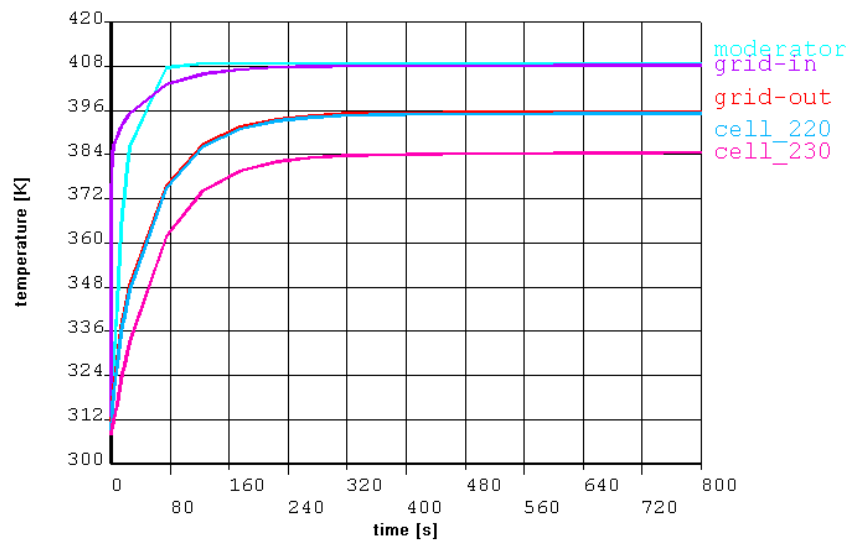


**Figure 13:** Temperature vs. time for different positions in the upper part of the lens and in the moderator; 1% beam power (diagnostic mode)

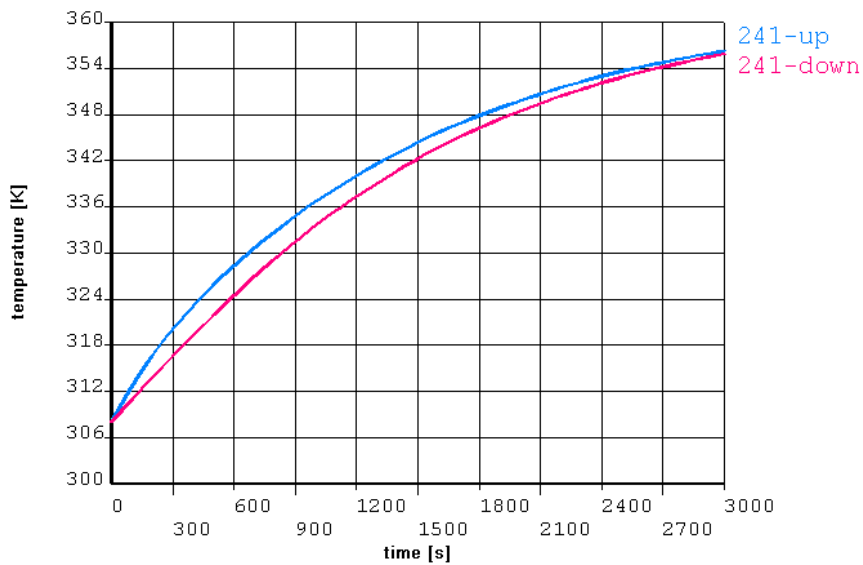


**Figure 14:** Temperature vs. time for different positions in the lower part of the lens; 1% beam power (diagnostic mode)

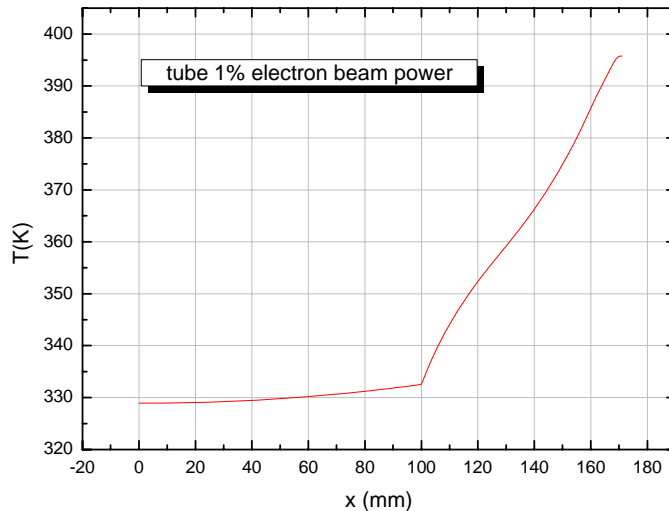


**Figure 15:** Temperature distribution [K] in the upper part of the extraction lens at  $t = 475$  s in the beam diagnostic mode (1% beam power). The left part of the tube ( $x=0\dots 100$ mm) has the full thickness (1mm). The right part ( $x > 100$ mm) has been thinned to a thickness of  $50 \mu\text{m}$  to reduce the power loss in the tube.

## 4 Conclusions

We performed a time-dependent thermal analysis of metallic parts (positron moderator and electrostatic extraction lens) of the positron source EPOS being directly exposed to the high-energetic, high-flux electron beam of the radiation source ELBE at the Research Center Dresden-Rossendorf. The temperature of the moderator can be adjusted by varying the thickness of the foil. It is possible to obtain high enough temperatures to ensure defect annealing under operation conditions. This will lead to a larger positron diffusion length, and thus to a higher efficiency of the electron-positron conversion. The extraction lens tube is made of stainless steel. The upper part which is hit by the high-intense electron beam must be thinned electrochemically in order to reduce the heat load. A version having a wall thickness of only  $50 \mu\text{m}$  has been realized and will be tested soon. We expect a temperature not higher than 1150 K. The mesh grid on top of the extraction tube which is also made from stainless steel will have a temperature of about 1100 K at full beam power. All this parts will be at a stable operation temperature after less than 60 s.

## References

- [1] R. Krause-Rehberg, H. S. Leipner, Positron Annihilation in Semiconductors, Vol. ISBN 3-540-64371-0 (Springer-Verlag, Berlin, 1999).
- [2] <http://www.fz-rossendorf.de/ELBE/> and <http://www.positronannihilation.net/EPOS/>
- [3] R. Krause-Rehberg, S. Sachert, G. Brauer, A. Rogov, K. Noack, Appl. Surf. Sci. 252, 3106 (2006).
- [4] MCNP – A General Monte Carlo N-Particle Transport Code, Version 5, X-5 Monte Carlo Team, LA-CP-03-0284, 2003.
- [5] Table of emissivity of various surfaces. Mikron Instrument Company, Inc.